

Dispersive Box Section and Its Applications to Quasi-TEM Mode Monoblock Dielectric Filters

Yan Zhang¹, Member, IEEE, Fabien Seyfert, and Ke-Li Wu², Fellow, IEEE

Abstract—In this article, the comprehensive theory for synthesis of a dispersive box coupling section for full control of two transmission zeros (TZs) is presented and applied to the design of high- Q monoblock dielectric resonator (MDR) filters. Compared to the traditional cascaded quadruplet (CQ) MDR section, the dispersive box section provides high flexibility in controlling TZs, a wide spurious free high rejection band, simplicity in physical realization, and higher unloaded Q s. The analytic transformation for converting a traditional CQ section with diagonal cross coupling to a dispersive box is given to facilitate the direct synthesis and justifies the uniqueness of the realizable solution to all possible TZ arrangements. Circuit realizations of all possible TZ arrangements are discussed with synthesized coupling matrices. A practical eight-pole MDR filter with an asymmetric response is synthesized and prototyped. Excellent agreement between the synthesized and measured narrowband responses as well as the EM simulated and measured wideband responses affirms the great flexibility in controlling TZs and demonstrates a wide spurious-free high rejection band with the proposed dispersive box structure. The low in-band insertion loss demonstrates that the MDR filter using the dispersive box can be potentially applied in 5G and future wireless communication systems.

Index Terms—Box section, cross coupling, dispersive coupling, monoblock dielectric resonator (MDR) filter, transmission zero (TZ).

I. INTRODUCTION

MONOBLOCK dielectric resonator (MDR) filters using quasi-TEM mode have regained high popularity recently for wireless communication systems employing the massive MIMO antenna array technology. MDR filters with comb-line structure using TEM mode resonators can be traced back to the 1980s [1], [2]. At that time, this kind of MDR filters could not replace the metal cavity coaxial resonator filters for wireless communication base stations due to their

Manuscript received 2 April 2022; revised 13 July 2022; accepted 15 October 2022. Date of publication 29 November 2022; date of current version 6 March 2023. This work was supported in part by the Research Grants Council of the Hong Kong Special Administrative Region, China, under Project CUHK 14208920; and in part by the Huawei Technologies Company Ltd. (Corresponding author: Ke-Li Wu.)

Yan Zhang was with the Department of Electronic Engineering, The Chinese University of Hong Kong, Shatin, Hong Kong. She is now with Huawei Technologies Company Ltd., Shanghai, China (e-mail: yzhang@link.cuhk.edu.hk).

Fabien Seyfert is with HighFSolutions, Nice, France (e-mail: fabien.seyfert@hfsolutions.fr).

Ke-Li Wu is with the Department of Electronic Engineering, The Chinese University of Hong Kong, Shatin, Hong Kong (e-mail: kluwu@cuhk.edu.hk).

Color versions of one or more figures in this article are available at <https://doi.org/10.1109/TMTT.2022.3222376>.

Digital Object Identifier 10.1109/TMTT.2022.3222376

0018-9480 © 2022 IEEE. Personal use is permitted, but republication/redistribution requires IEEE permission.

See <https://www.ieee.org/publications/rights/index.html> for more information.

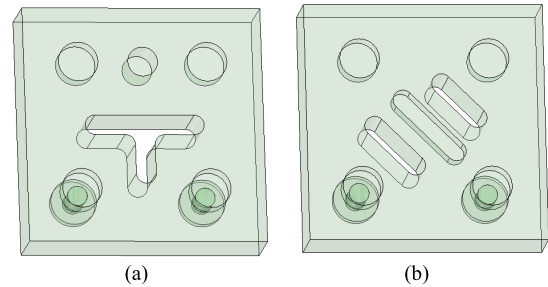


Fig. 1. Existing physical structures of quadruplet section in MDR filters. (a) Quadruplet without diagonal cross coupling. (b) Quadruplet with diagonal cross coupling.

low quality factor Q despite their great compactness. MDR filters using high Q waveguide resonators were proposed in the 1990s [3], [4] and further studied in recent years [5]. These works are rarely used in wireless communication systems due to their relatively bulky size and the difficulty of introducing transmission zeros (TZs) in a monoblock structure. A TM_{01} mode MDR filter is introduced in [6] using the resonator with a dielectric rod of one open- and one short-circuited ends. Compared to a metal cavity coaxial resonator filter, higher Q is achieved, yet the size is comparable.

A good compromise of compact size, low insertion loss, and high rejection, which are the three basic requirements for filters in a wireless communication system, is achieved for an MDR filter in [7]. In an MDR filter, the waveguide resonator is loaded by a metalized cylindrical ridge or the partial height blind hole depressed from the top, which reduces the size of the resonator and supports the quasi-TEM mode. Most essentially, the resonator allows more flexibilities in coupling layout for creating TZs while maintaining an overall cuboid shape of the filter, which is a necessity for maximizing unloaded Q and being compatible with the stamping press fabrication process.

The MDR filter with quasi-TEM mode resonators comes along with more rigid design rules in resonator layout compared with metal coaxial resonator filters. The two most favorably used sections for generating TZs, namely, cascaded triplet (CT) and cascade quadruplet (CQ) [8], become difficult to implement in MDR filters due to manufacturing inconvenience and spurious mode constraints. Fig. 1 shows two existing realizations of a CQ section, among which the most popular one is shown in Fig. 1(a) that creates two TZs with one in low and one in high rejection bands. The required

negative coupling is realized by the metalized blind hole [7]. Due to the dispersion effect of the blind hole, the two TZs are asymmetric, and their locations can hardly be independently controlled.

One way to realize a diagonal cross coupling to control the two TZs is to use a diagonal ridge together with two partition walls, as shown in Fig. 1(b) [9]. Apart from the complexity of the structure, which may lower the unloaded Q of the related resonators and its strong dispersion effect, the diagonal ridge generates the spurious mode in the high rejection band that is lower than the first higher order mode of the resonator.

It is known that the quadruplet section shown in Fig. 1(b) creates two TZs on the same side of the passband if all the couplings between each pair of adjacent resonators are positive, whereas the sign of the diagonal cross coupling controlled by the depth of the diagonal ridge decides which side they are on. To create two TZs on each side of the passband, a metalized blind hole needs to be placed at one of the four positions between two adjacent resonators in a very congregated space. In such a circumstance, the physical structure of the quadruplet section becomes very complicated to design and fabricate. Therefore, it would be desirable to find a simpler CQ-like coupling structure that is able to fully control the two TZs.

Prior to the use in MDR filters as a negative coupling element, the metalized blind hole was first applied in waveguide filters as a partial height post-coupling element with a band-rejection characteristic [10]. In [11], [12], and [13], the structure is considered as a dispersive coupling element. The simplest coupling topology with a dispersive coupling is a duplet section that can generate one TZ [14]. In recent years, considerable efforts have been devoted to synthesizing bandpass filters with dispersive coupling elements [15], [16], [17]. A general folded topology with dispersive couplings is introduced in [18]. It is revealed that dispersive coupling can replace the diagonal cross coupling in a traditional folded form. The direct synthesis method of several most useful coupling sections, i.e., duplets, triplets, and quadruplets, with dispersive couplings is proposed very recently in [19] together with the shortest path rule for the coupled-resonator filters with dispersive coupling elements.

Besides the CQ section, the quadruplet box section without diagonal cross coupling can also generate two TZs when one of the mutual couplings is dispersive according to the shortest path rule. Such a box section with a dispersive coupling will be called “dispersive box” for brevity. The dispersive box topology is first utilized to design a four-pole substrate integrated waveguide filter with two TZs in the high rejection band only [20]. The work demonstrates that a dispersive coupling in a dispersive box can generate one more TZ than a regular box section [21] without providing a theoretic explanation. Similar applications of a dispersive coupling to generate an extra TZ in a box or an extended box section are also reported recently in [22] and [23]. However, the full potential of the dispersive box has not been explored yet.

The traditional box coupling topology without diagonal cross coupling is not popularly used in filter designs for wireless applications for a number of reasons, among which

creating fewer TZs compared to a quadruplet section and its multiple-solution issue [24] are two major ones. Despite the shortcomings, it will be shown in this article that when a dispersive box section is used in an MDR filter, two TZs can be easily realized, flexibly arranged, and fully controlled without arousing the near-passband spurious mode. In particular, the dispersive box section makes it possible to realize and control two TZs on one side of the passband while maintaining a wide spurious free rejection band, which is very difficult to achieve with an MDR quadruplet section. Such a TZ arrangement is especially significant in designing diplexers to ensure sufficient channel isolation.

In this article, a novel coupling structure for quasi-TEM mode MDR filters, namely, dispersive box, is introduced. The dispersive box can provide two fully controllable TZs. This unique feature leads to a wide spurious-free high rejection band, simplicity in realization, and higher unloaded Q . The analytic transformation for converting a traditional CQ section to a dispersive box is also developed. The closed-form transformation facilitates the direct synthesis and justifies the existence of the unique realizable solution to all possible TZ arrangements. A practical asymmetric eight-pole MDR filter composed of two cascaded dispersive boxes is synthesized, EM designed, and prototyped. Excellent agreement is achieved between the synthesized and measured narrowband responses as well as the EM simulated and measured wideband responses.

II. COUPLING MATRIX OF DISPERSIVE BOX

It is known that the admittance matrix of a dispersion-less coupled-resonator network can be written as [22]

$$\mathbf{Y} = -j\mathbf{B}^T(\mathbf{M} + \omega\mathbf{I})^{-1}\mathbf{B} \quad (1)$$

where ω is the low-pass frequency. The circuit model is represented by $(\mathbf{I}, \mathbf{M}, \mathbf{B})$, where \mathbf{I} is an $N \times N$ identity matrix, \mathbf{M} is an $N \times N$ matrix whose elements represent couplings between resonators and self-couplings, and \mathbf{B} is an $N \times 2$ matrix consisting of couplings between input–output (I/O) and resonators. By applying the congruent transform to the circuit model, a dispersive coupled-resonator network with the same response represented by $(\mathbf{M}_d, \mathbf{M}_0, \mathbf{B}')$ can be obtained with the corresponding admittance matrix reexpressed as

$$\mathbf{Y} = -j\mathbf{B}'^T(\mathbf{M}_0 + \omega\mathbf{M}_d)^{-1}\mathbf{B}' \quad (2a)$$

where

$$\mathbf{M}_0 = \mathbf{Q}\mathbf{M}\mathbf{Q}^T, \quad \mathbf{M}_d = \mathbf{Q}\mathbf{Q}^T, \quad \mathbf{B}' = \mathbf{Q}\mathbf{B} \quad (2b)$$

with \mathbf{Q} being nonsingular. Although the topology of \mathbf{M} in (1) can be arbitrary, this work will focus on the transformation from a traditional CQ section with diagonal cross coupling to a dispersive box to reveal the essence of the two solutions.

Starting from the traditional CQ section shown in Fig. 2(a) that realizes two TZs of an arbitrary arrangement, the coupling matrix for the quasi-box topology shown in Fig. 2(b) can be

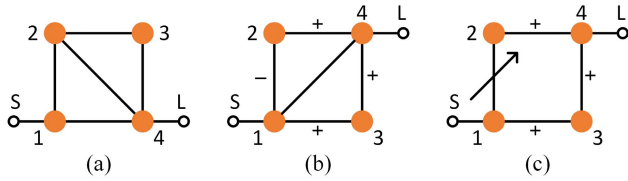


Fig. 2. Three equivalent quadruplet topologies in (a) CQ form with diagonal cross coupling, (b) quasi-box form with diagonal cross coupling, and (c) dispersive box form with dispersive coupling (1–2).

obtained by a similarity transformation with pivot $[i, j] = [2, 3]$ and the rotation angle of [21]

$$\theta_r = \frac{1}{2} \tan^{-1} \left(\frac{2M_{ij}}{M_{jj} - M_{ii}} \right). \quad (3)$$

It is called quasi-box here as there is an extra coupling (1–4) compared to the regular box topology. It will be shown in the appendix that, under the mild hypothesis that none of the TZs of the quasi-box section lies in between two resonant frequencies, one of the mutual couplings (except M_{14}) must be with a different sign from the others. Irrespective of the sign of the cross coupling (1–4) in Fig. 2(b), coupling (1–2) is chosen to be negative with the other three couplings being positive.

The two solutions of this topology can be obtained with two possible rotation angles resulting from (3), which can also be obtained from the antisymmetry of the quasi-box structure. Note that the structure in Fig. 2(b) is symmetric in the sense that exchanging of resonators 2 and 3 results in an unchanged topology. Therefore, the second solution $\mathbf{M}^{(2)}$ can be observed based on a permutation of the first solution $\mathbf{M}^{(1)}$ by

$$\begin{aligned} \mathbf{M}^{(2)} &= \mathbf{P}\mathbf{M}^{(1)}\mathbf{P}^T \\ &= \begin{pmatrix} M_{11}^{(1)} & -M_{13}^{(1)} & -M_{12}^{(1)} & -M_{14}^{(1)} \\ -M_{13}^{(1)} & M_{33}^{(1)} & 0 & M_{34}^{(1)} \\ -M_{12}^{(1)} & 0 & M_{22}^{(1)} & M_{24}^{(1)} \\ -M_{14}^{(1)} & M_{34}^{(1)} & M_{24}^{(1)} & M_{44}^{(1)} \end{pmatrix} \end{aligned} \quad (4a)$$

with the permutation matrix being

$$\mathbf{P} = \begin{bmatrix} -1 & 0 & 0 & 0 \\ 0 & 0 & 1 & 0 \\ 0 & 1 & 0 & 0 \\ 0 & 0 & 0 & 1 \end{bmatrix}. \quad (4b)$$

Note that the sign change for the first row and column is for maintaining the negative sign of coupling (1–2) in Fig. 2(b). Neglecting the polarity of M_{14} , suppose that $M_{(12)}^{(1)}$ is negative and all other couplings are positive, and the permutation would result in a similar polarity with $M_{(12)}^{(2)}$ being negative and all other couplings being positive. Obviously, by maintaining a consistent polarity of the coupling between two adjacent resonators, the polarity of the cross coupling M_{14} will be reversed after the permutation. This is the key point for all realizable responses and will be further illustrated in detail.

To transform the quasi-box topology to the dispersive box topology in Fig. 2(c), one can analytically solve the polynomial system equations by enforcing the unwanted elements in

the coupling matrix in (2b) to be zero. Specifically, if only coupling (1–2) is designated to be a dispersive element, the polynomial equations can be formulated as

$$\begin{cases} (\mathbf{QM}\mathbf{Q}^T)_{i,j} = 0, & \text{for } (i, j) = \{(2, 3), (1, 4)\} \\ (\mathbf{Q}\mathbf{Q}^T)_{i,j} = 0, & \text{for } (i, j) \\ & = \{(1, 3), (1, 4), (2, 3), (2, 4), (3, 4)\} \\ (\mathbf{Q}\mathbf{Q}^T)_{i,i} = 1, & \text{for } i = 1, \dots, 4 \\ (\mathbf{Q}\mathbf{B})_{i,j} = 0, & \text{for } (i, j) \\ & = \{(S, 2), (S, 3), (S, 4), (1, L), (2, L), (3, L)\} \end{cases} \quad (5)$$

with \mathbf{Q} being the unknown and presumably non-singular and $(\mathbf{I}, \mathbf{M}, \mathbf{B})$ being the dispersion-less coupling matrix of the quasi-box section.

Regardless of the other aforementioned solution by permutation, the unique solution to (5) can be found as

$$\mathbf{Q} = \begin{pmatrix} \frac{-M_{24}}{\sqrt{M_{14}^2 + M_{24}^2}} & \frac{M_{14}}{\sqrt{M_{14}^2 + M_{24}^2}} & & \\ & -1 & & \\ & & -1 & \\ & & & -1 \end{pmatrix}$$

with all other entries being zeros, resulting in the dispersive coupling matrix $(\mathbf{M}_d, \mathbf{M}_0, \mathbf{B}')$

$$M_d(1, 2) = \frac{-M_{14}}{\sqrt{M_{14}^2 + M_{24}^2}} \quad (6a)$$

$$M_0(1, 1) = \frac{M_{22}M_{14}^2 - 2M_{12}M_{14}M_{24} + M_{11}M_{24}^2}{M_{14}^2 + M_{24}^2}$$

$$M_0(2, 2) = M_{22}$$

$$M_0(1, 2) = \frac{M_{12}M_{24} - M_{14}M_{22}}{\sqrt{M_{14}^2 + M_{24}^2}}$$

$$M_0(2, 4) = M_{24}, \quad M_0(3, 3) = M_{33}$$

$$M_0(1, 3) = \frac{M_{13}M_{24}}{\sqrt{M_{14}^2 + M_{24}^2}}, \quad M_0(3, 4) = M_{34}$$

$$M_0(4, 4) = M_{44}$$

(6b)

and

$$B'(1, 1) = \frac{M_{24}M_{S1}}{\sqrt{M_{14}^2 + M_{24}^2}}, \quad B'(4, 1) = M_{4L} \quad (6c)$$

where $B(1, 1) = M_{S1}$ and $B(2, 4) = M_{4L}$ are the I/O couplings in the quasi-box topology. Since both M_{13} and M_{24} are positive, $M_0(1, 3)$, as well as the unchanged $M_0(2, 4)$ and $M_0(3, 4)$, are also positive. As for the slope of the dispersive coupling (1–2), its polarity is opposite to that of M_{14} according to (6a). It will be shown in the next section that the dispersive coupling realized by a blind hole always holds a positive M_d . In this regard, when the synthesized $M_d(1, 2)$ is negative and is unrealizable in MDR filters, the sign of M_{14} needs to be reversed by the permutation in (4) to pick the other solution to ensure that $M_d(1, 2)$ is always realizable. In conclusion, the dispersive box has one and only one realizable solution for MDR filters. The hassle caused by

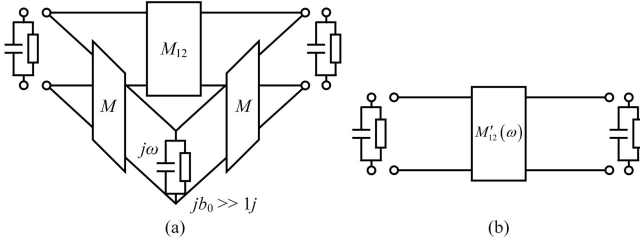


Fig. 3. Equivalent circuits of the blind coupling hole between two adjacent resonators in Fig. 1(a). (a) Two resonators are coupled to each other and both coupled to the blind hole, which is considered as a resonator whose resonating frequency is much lower than the passband. (b) Aggregated dispersive inverter.

the multiple solutions of a box topology turns out to be an advantage in both design and tuning of MDR filters.

III. REALIZATION OF THE DISPERSIVE BOX SECTION

A. Theoretical Analysis of the Blind Coupling Hole

Physically, the blind coupling hole itself is a resonator with a much lower frequency than the interested frequency band as shown in [22]. The physical circuit model of two adjacent resonators coupled with a blind hole is shown in Fig. 3(a), where the adjacent resonators are not only coupled to each other with inverter M_{12} but also both coupled to the blind hole resonator with inverters M . The frequency invariant reactance b_0 of the blind hole is much larger than 1 since its frequency is much lower than the passband.

By circuit analysis or (1), the admittance matrix of the two adjacent resonators coupled with a blind hole can be easily obtained as

$$\mathbf{Y} = \begin{bmatrix} \frac{M^2}{j\omega + jb_0} & \frac{M^2}{j\omega + jb_0} \\ \frac{M^2}{j\omega + jb_0} & \frac{M^2}{j\omega + jb_0} \end{bmatrix} + \begin{bmatrix} 0 & jM_{12} \\ jM_{12} & 0 \end{bmatrix}$$

$$= \begin{bmatrix} 0 & jM_{12} - j\frac{M^2}{\omega + b_0} \\ jM_{12} - j\frac{M^2}{\omega + b_0} & 0 \end{bmatrix} + \begin{bmatrix} \frac{M^2}{j\omega + jb_0} & 0 \\ 0 & \frac{M^2}{j\omega + jb_0} \end{bmatrix} \quad (7)$$

where the diagonal terms can be absorbed into the adjacent resonators and the off-diagonal terms can then be considered as the aggregated coupling $M'_{12}(\omega)$ in Fig. 3(b), which is

$$M'_{12}(\omega) = jM_{12} - j\frac{M^2}{\omega + b_0}$$

$$= jM_{12} - j\left(\frac{M^2}{b_0} - \frac{M^2}{b_0^2}\omega + \frac{M^2}{b_0} \sum_{k=2}^{\infty} \left(\frac{\omega}{-b_0}\right)^k\right)$$

$$\approx j\left(M_{12} - \frac{M^2}{b_0} + \frac{M^2}{b_0^2}\omega\right)$$

$$= j(M_0 + M_d\omega) \quad (8)$$

where the high-order terms in the power series are discarded since $b_0 \gg 1$. The positive nature of the dispersive slope is revealed by

$$M_d = M^2/b_0^2. \quad (9)$$

This property was first exposed in [22] and will further be verified in the following section.

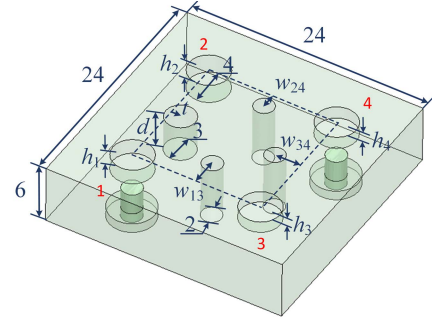


Fig. 4. Physical structure and dimensions of a typical MDR dispersive box with the dispersive coupling realized by a blind hole between resonators 1 and 2, and other positive couplings realized by through holes (unit: mm).

TABLE I

DIMENSIONS OF THE DISPERSIVE BOX FILTER UTILIZED FOR DISPERSIVE COUPLING ANALYSIS (UNIT: MM)

h_1	h_2	h_3	h_4	w_{13}	w_{24}	w_{34}
1.5	2	1.2	1.5	2.5	2.5	2.5

B. Analysis of the Dispersive Coupling in the Dispersive Box

A typical realization of the proposed dispersive box section in the context of MDR filters is shown in Fig. 4. Considering the manufacturing constraints on the thickness of the ceramic wall between the blind hole and the air walls for partition of resonators as shown in Fig. 1, metalized through holes are utilized instead. It is worth mentioning that this slight change in the structure for positive couplings does not affect the characteristics of the coupling.

To give a flavor of the dispersion characteristic of a typical blind hole for realizing a negative coupling in an MDR filter, the dispersive box shown in Fig. 4 is EM analyzed with reference to the center frequency $f_0 = 3.6$ GHz and the bandwidth $BW = 0.2$ GHz. The dimensions of the structure are listed in Table I and the relative permittivity of the ceramic block is 19.15. To rule out the nonphysical solution during the analysis, the heights h_2 and h_3 of the cylindrical ridges on top of resonators 2 and 3 are deliberately set to be distinguishable. According to (4) and (6), two self-couplings (M_{22} and M_{33}) are exchanged in the two solutions, which is a useful feature to distinguish one solution from the other.

By extracting the coupling matrix from the response of the four-pole structure and using the transformation in (4) and (6), the slope and the constant part of dispersive coupling (1–2) can be obtained. There are two mathematical solutions according to the discussion in Section II, only the one that corresponds to the physical realization is presented in Fig. 5, in which the slope $M_d(1, 2)$ and constant part $M_0(1, 2)$ are studied with respect to the offset t and depth d of the blind hole. The offset t is the distance from the center-to-center line of resonators 1 and 2 to the center of the blind hole. t is positive (negative) when close to the center (outside wall) of the block. It can be observed that the constant part M_0 becomes minimum at $t = 0$, which is similar to the characteristic of the positive coupling through hole. It is observed that M_0 can vary in a

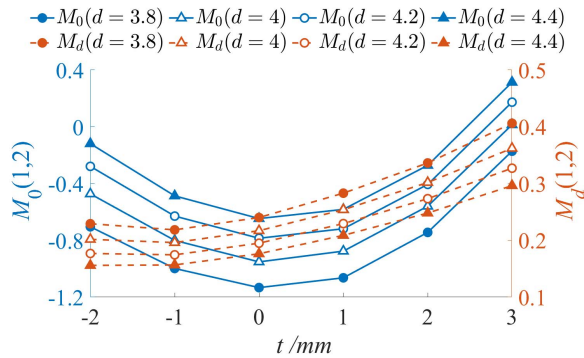


Fig. 5. Constant part M_0 and the slope M_d of the dispersive coupling (1–2) versus offset t and depth d of the blind hole.

wide range by adjusting the offset t . This feature is critical in flexibly arranging and controlling TZs by a dispersive box section.

Fig. 5 also shows that the dispersive slope M_d increases monotonously with the increase of t . The increase of the depth d leads to decreasing M_d and increasing M_0 , providing a wide range of combination of M_d and M_0 . It is worth noting that M_d is always positive for the blind hole structure, which supports the conclusion in Section II that the dispersive box topology has only one solution that is realizable for MDR filters.

IV. ARRANGEMENT AND CONTROL OF TZS

In this section, six TZ arrangements that are realizable by a dispersive box will be discussed through the synthesis of six four-pole filters with the passband centered at $f_0 = 3.6$ GHz and the bandwidth $BW = 0.2$ GHz for 22 dB return loss. The six TZ arrangements cover all possible needs for a quadruplet section with two TZs. The detailed analytic synthesis process will be illustrated in the first example. In the second example, the advantage of using dispersive box section is demonstrated by comparing the physical realizations of dispersive box with the traditional CQ using a ridge for diagonal cross coupling in an MDR filter. The following three examples exhibit the benefits of the dispersive box over the dispersive quadruplet without diagonal cross coupling in the context of MDR filters. The response with a pair of complex conjugated TZs for equalized in-band group delay is realized in the last example.

A. TZ Arrangement 1: Two TZs in Low Rejection Band

Assume that two TZs are assigned in the low rejection band whose normalized zero frequencies in the low-pass frequency domain are located at $-2.8j$ and $-1.6j$. This response cannot be realized by the existing quadruplet structure shown in Fig. 1(a) since the synthesized coupling matrix as shown in the following has a nonzero diagonal cross coupling

$$\mathbf{M} = \begin{pmatrix} 0 & 1.0882 & 0 & 0 & 0 & 0 \\ 1.0882 & -0.1074 & 0.9732 & 0 & 0.1717 & 0 \\ 0 & 0.9732 & -0.0248 & 0.4534 & -0.6439 & 0 \\ 0 & 0 & 0.4534 & 0.7753 & 0.7298 & 0 \\ 0 & 0.1717 & -0.6439 & 0.7298 & -0.1074 & 1.0882 \\ 0 & 0 & 0 & 0 & 1.0882 & 0 \end{pmatrix}.$$

TABLE II

DIMENSIONS OF THE DISPERSIVE BOX FILTER WITH TWO TZS IN LOW REJECTION BAND (UNIT: MM)

h_1	h_2	h_3	h_4	w_{13}	w_{24}	w_{34}	t	d
1.55	1.91	1.19	1.395	2.71	1.7	2.46	2.5	4.46

For this response, the resonating frequencies are $\omega = [1.5090 \ 0.2060 - 1.0005 - 1.2502]$. The TZs are both smaller than the minimal resonating frequency $\omega = -1.2502$ and the condition in the Appendix is satisfied.

As shown in the following transformation, M_{12} is negative and M_{13} , M_{24} , and M_{34} are all positive in the quasi-box topology. With $\theta_r = 0.4239$ rad, \mathbf{M} can be transformed to the quasi-box topology. After the permutation in (4), the coupling matrix can be reexpressed as

$$\mathbf{M} = \begin{pmatrix} 0 & 1.0882 & 0 & 0 & 0 & 0 \\ 1.0882 & -0.1074 & -0.4003 & 0.8871 & -0.1717 & 0 \\ 0 & -0.4003 & 0.9799 & 0 & 0.4003 & 0 \\ 0 & 0.8871 & 0 & -0.2294 & 0.8871 & 0 \\ 0 & -0.1717 & 0.4003 & 0.8871 & -0.1074 & 1.0882 \\ 0 & 0 & 0 & 0 & 1.0882 & 0 \end{pmatrix}.$$

For simplicity, the $N \times N$ matrix \mathbf{M} and the $N \times 2$ matrix \mathbf{B} in Section II are combined to form the $(N + 2) \times (N + 2)$ matrix \mathbf{M} , where the first and last rows and columns represent the couplings associated with I/O ports, respectively. Note that only the solution with a negative M_{14} is selected and presented here.

Then, the dispersive coupling matrix in the dispersive box topology can be obtained by (6) with the dispersive slope $M_d(1, 2) = 0.3942$, which is realizable in an MDR filter. The corresponding constant coupling matrix of the dispersive box is

$$\mathbf{M}_0 = \begin{pmatrix} 0 & 1.0001 & 0 & 0 & 0 & 0 \\ 1.0001 & -0.2285 & 0.0184 & 0.8152 & 0 & 0 \\ 0 & 0.0184 & 0.9799 & 0 & 0.4003 & 0 \\ 0 & 0.8152 & 0 & -0.2294 & 0.8871 & 0 \\ 0 & 0 & 0.4003 & 0.8871 & -0.1074 & 1.0882 \\ 0 & 0 & 0 & 0 & 1.0882 & 0 \end{pmatrix}.$$

The physical realization of the synthesized dispersive box filter is EM designed with the structure same as that shown in Fig. 4 and the dimensions are listed in Table II. The responses of the EM designed and the synthesized dispersive coupling matrix are superimposed in Fig. 6. The nice fitness demonstrates that the synthesized circuit model of the dispersive box is physically realizable and can effectively guide the physical design.

B. TZ Arrangement 2: Two TZs in High Rejection Band

Assigning two TZs in the high rejection band at $+1.5j$ and $+2.3j$, the condition for the TZs is satisfied as the maximal resonating frequency is found to be 1.2332. Following the same synthesis process, the dispersive coupling matrix of

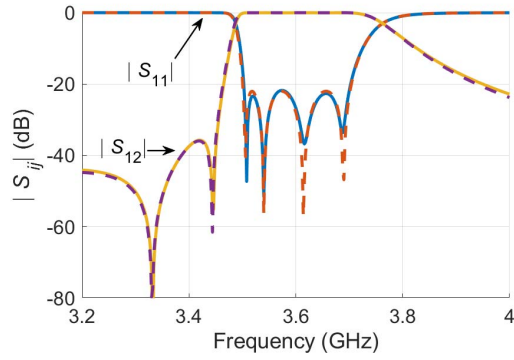


Fig. 6. Responses of synthesized dispersive coupling matrix (dashed lines) and the EM model (solid lines) of a dispersive box with two TZs in low rejection band (TZ arrangement 1).

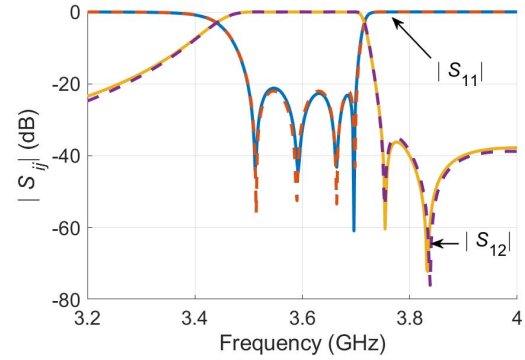


Fig. 8. Responses of synthesized dispersive coupling matrix (dashed lines) and EM model (solid lines) of a dispersive box with two TZs in high rejection band (TZ arrangement 2).

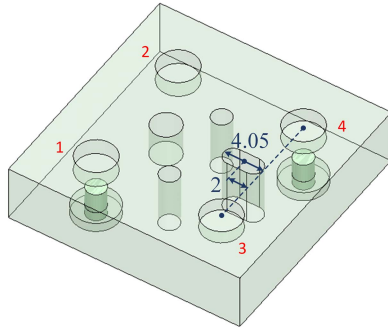


Fig. 7. Physical structure of a dispersive box realizing two TZs in high rejection band (unit: mm).

TABLE III

DIMENSIONS OF THE DISPERSIVE BOX FILTER WITH TWO TZS IN HIGH REJECTION BAND (UNIT: MM)

h_1	h_2	h_3	h_4	w_{13}	w_{24}	t	d
1.732	1.693	1.393	1.497	1.68	3.05	3	3.57

the dispersive box can be synthesized as

$$M_0 = \begin{pmatrix} 0 & 1.0567 & 0 & 0 & 0 & 0 \\ 1.0567 & -0.3085 & -0.8387 & 0.3541 & 0 & 0 \\ 0 & -0.8387 & 0.1385 & 0 & 0.9011 & 0 \\ 0 & 0.3541 & 0 & -0.9959 & 0.3655 & 0 \\ 0 & 0 & 0.9011 & 0.3655 & 0.1233 & 1.0908 \\ 0 & 0 & 0 & 0 & 1.0908 & 0 \end{pmatrix}$$

with $M_d(1, 2) = 0.2479$. Again, this response with two TZs on one side of the passband cannot be realized by the existing CQ structure without using diagonal cross coupling.

The structure of the EM designed filter is shown in Fig. 7, which is slightly different from that in Fig. 4 in that the through hole for realizing coupling (3–4) is extended to an air wall for the weak coupling. The air wall is centered 2 mm away from the center-to-center line of resonators 3 and 4 with the width of 4.05 mm. The other dimensions of the filter are listed in Table III and the synthesized and EM simulated responses are plotted in Fig. 8, showing excellent agreement again.

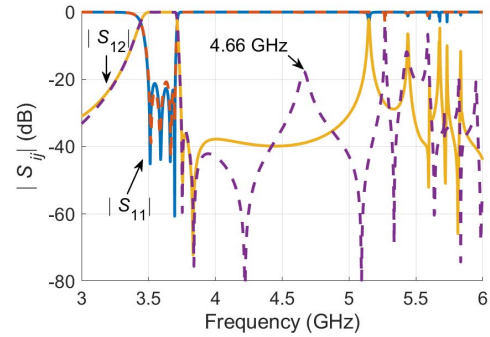


Fig. 9. Wideband responses of traditional quadruplet with diagonal cross coupling as shown in Fig. 1(b) (dashed lines) and the dispersive box shown in Fig. 7 (solid lines).

It is reported in [9] that the structure shown in Fig. 1(b) can also realize a response with two TZs on the same side. In this case, a diagonal ridge with two air walls on the two sides must be introduced for the necessary diagonal cross coupling. The physical realization using the structure in Fig. 1(b) that achieves the same response as that shown in Fig. 8 is also EM designed, whose wideband response is plotted in dashed lines in Fig. 9. For comparison, the wideband response of the EM designed MDR filter in Fig. 7 is superimposed in Fig. 9 in solid lines. It can be seen that the spurious mode due to the diagonal ridge of the quadruplet structure at 4.66 GHz is disappeared in the response of the filter with dispersive box configuration, leaving a wide spurious mode free rejection band.

Besides, the two diagonal air walls in the CQ structure will introduce additional losses to the two concerned resonators, lowering the unloaded Q . Supposing that the conductivity of the silver coating layer outside the MDR filter is 4.5×10^7 S/m and the loss tangent of the dielectric is 5×10^{-5} , the unloaded Q of each resonator of the filter in Fig. 7 is found by vector fitting as [25]

$$Q_1 = [1734 \ 1796 \ 1861 \ 1783].$$

On the other hand, for the filter using a CQ section with two diagonal air walls, the extracted unloaded Q of each resonator is found as

$$Q_2 = [1601 \ 1784 \ 1632 \ 1740]$$

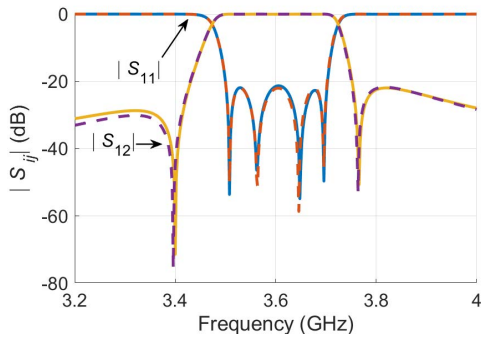


Fig. 10. Responses of synthesized dispersive coupling matrix (dashed lines) and EM model (solid lines) of a dispersive box with one far TZ in low and one close TZ in high rejection bands (TZ arrangement 3).

TABLE IV

DIMENSIONS OF THE DISPERSIVE BOX FILTER WITH ONE FAR TZ IN LOW REJECTION BAND AND ONE CLOSE TZ IN HIGH REJECTION BAND (UNIT: MM)

h_1	h_2	h_3	h_4	w_{13}	w_{24}	w_{34}	t	d
1.638	1.548	1.522	1.432	2.47	2.07	2.26	3	3.6

where Q_s of resonators 1 and 3 are obviously deteriorated.

Apart from spurious mode and extra loss, the complex structure will further bring more fabrication uncertainties than the proposed dispersive box structure.

C. TZ Arrangement 3: One TZ in Low and One Close TZ in High Rejection Bands

According to the analysis in Section III, the blind hole introduces a dispersive coupling with a positive slope, which leads to an asymmetry of the response with one far TZ in the low rejection band and one closer to the passband TZ in the high rejection band when existing CQ shown in Fig. 1(a) is used to generate two TZs in both rejection bands. Such a response can also be realized by the dispersive box structure.

Assigning two TZs at $+1.6j$ and $-2.1j$, the condition for the TZs is satisfied because the interval spanned by the resonating frequencies is found to be $[-1.354, 1.2953]$. The dispersive coupling matrix can be directly synthesized as

$$\mathbf{M}_0 = \begin{pmatrix} 0 & 0.9783 & 0 & 0 & 0 & 0 \\ 0.9783 & -0.5391 & -0.8711 & 0.6358 & 0 & 0 \\ 0 & -0.8711 & -0.8780 & 0 & 0.5699 & 0 \\ 0 & 0.6358 & 0 & 0.7492 & 0.6924 & 0 \\ 0 & 0 & 0.5699 & 0.6924 & 0.0156 & 1.0654 \\ 0 & 0 & 0 & 0 & 1.0654 & 0 \end{pmatrix}$$

where $M_d(1, 2) = 0.3961$. The structure of the EM designed filter is the same as that in Fig. 4 and the dimensions are listed in Table IV. The responses of the EM simulated and the synthesized filter are superposed in Fig. 10, also showing excellent agreement.

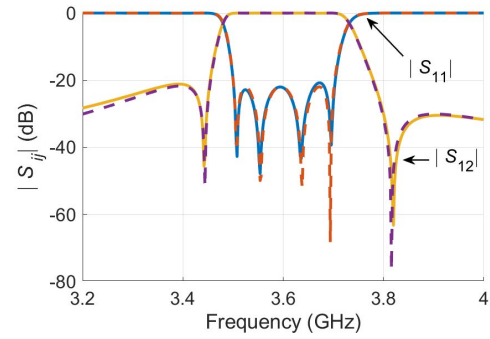


Fig. 11. Responses of synthesized dispersive coupling matrix (dashed lines) and EM model (solid lines) of a dispersive box with one far TZ in high and one close TZ in low rejection bands (TZ arrangement 4).

TABLE V

DIMENSIONS OF THE DISPERSIVE BOX FILTER WITH ONE FAR TZ IN HIGH REJECTION BAND AND ONE CLOSE TZ IN LOW REJECTION BAND (UNIT: MM)

h_1	h_2	h_3	h_4	w_{13}	w_{24}	w_{34}	t	d
1.69	1.57	1.618	1.42	2.17	2.38	2	2.9	3.55

D. TZ Arrangement 4: One Close TZ in Low and One TZ in High Rejection Bands

Opposite to TZ arrangement 3, the response, in this case, has one TZ that is close to the passband in the low rejection band. Such a response is impossible to be realized by the regular MDR quadruplet structure shown in Fig. 1(a) since a dispersive coupling with a negative slope is required otherwise, which is difficult to realize with the blind hole structure according to the analysis in Section III.

Assuming that the two TZs to be realized are $-1.6j$ and $+2.1j$ in the low-pass frequency domain, again, the condition for the TZs is satisfied because the interval spanned by the resonating frequencies is found to be $[-1.2953, 1.354]$. The synthesized dispersive coupling matrix can be found as

$$\mathbf{M}_0 = \begin{pmatrix} 0 & 1.0040 & 0 & 0 & 0 & 0 \\ 1.0040 & -0.5343 & -0.9032 & 0.5371 & 0 & 0 \\ 0 & -0.9032 & -0.7492 & 0 & 0.6924 & 0 \\ 0 & 0.5371 & 0 & 0.8780 & 0.5699 & 0 \\ 0 & 0 & 0.6924 & 0.5699 & -0.0156 & 1.0654 \\ 0 & 0 & 0 & 0 & 1.0654 & 0 \end{pmatrix}$$

where $M_d(1, 2) = 0.3346$. The structure in Fig. 4 is used again with dimensions listed in Table V. Responses by the EM simulated and synthesized filters are superposed in Fig. 11.

E. TZ Arrangement 5: Response With Two Symmetric TZs

This is another useful filter response that can hardly be realized by the regular MDR quadruplet in Fig. 1(a). As previously explained, the response with two symmetric TZs is also unrealizable by an MDR quadruplet since the required dispersive slope in this case is 0, which is unattainable for a blind hole. It will be shown that the dispersive box can easily achieve the symmetric response. For two symmetric

TABLE VI
DIMENSIONS OF THE DISPERSIVE BOX FILTER WITH
TWO SYMMETRIC TZS (UNIT: MM)

h_1	h_2	h_3	h_4	w_{13}	w_{24}	w_{34}	t	d
1.617	1.527	1.567	1.419	2.37	2.31	2.17	3.7	3.3

TABLE VII
DIMENSIONS OF THE DISPERSIVE BOX FILTER WITH
TWO COMPLEX CONJUGATED TZS (UNIT: MM)

h_1	h_2	h_3	h_4	w_{13}	w_{24}	w_{34}	t	d
1.71	1.87	1.22	1.39	2.25	2.48	1.93	2	4.28

TZs at $\pm 1.6j$, which is outside of the resonating frequency range $[-1.3015, 1.3015]$, the dispersive coupling matrix can be synthesized as

$$\mathbf{M}_0 = \begin{pmatrix} 0 & 0.9238 & 0 & 0 & 0 & 0 \\ 0.9238 & -0.7265 & -0.9484 & 0.5309 & 0 & 0 \\ 0 & -0.9484 & -0.8499 & 0 & 0.6095 & 0 \\ 0 & 0.5309 & 0 & 0.8499 & 0.6095 & 0 \\ 0 & 0 & 0.6095 & 0.6095 & 0 & 1.0605 \\ 0 & 0 & 0 & 0 & 1.0605 & 0 \end{pmatrix}$$

where $M_d(1, 2) = 0.4911$.

The dimensions of the EM-designed filter are listed in Table VI. Note that the required M_d is large in this case yet still physically realizable since the through holes are utilized to replace the air partition walls so that the blind hole will not conflict with air walls. The EM simulated and synthesized responses are plotted in Fig. 12 with excellent agreement.

F. TZ Arrangement 6: Response With Complex Conjugated TZs

Last but not least, the response with two complex conjugated TZs $\pm 2 + 0.1j$ is considered in this case for equalized in-band group delay. The synthesized coupling matrix can be found as

$$\mathbf{M}_0 = \begin{pmatrix} 0 & 1.0719 & 0 & 0 & 0 & 0 \\ 1.0719 & -0.2485 & -0.5571 & 0.6725 & 0 & 0 \\ 0 & -0.5571 & 0.6561 & 0 & 0.7046 & 0 \\ 0 & 0.6725 & 0 & -0.6855 & 0.6867 & 0 \\ 0 & 0 & 0.7046 & 0.6867 & 0.0042 & 1.0945 \\ 0 & 0 & 0 & 0 & 1.0945 & 0 \end{pmatrix}$$

where $M_d(1, 2) = 0.2025$.

Although the required dispersion effect is weaker than in previous cases, it is still realizable with the dimensions listed in Table VII. Both the magnitude and group delay responses of the EM simulation demonstrate good fitness with the synthesized result in Fig. 13.

V. PRACTICAL DESIGN EXAMPLE

In this section, an eight-pole MDR filter in the coupling structure of two cascaded dispersive box sections is designed

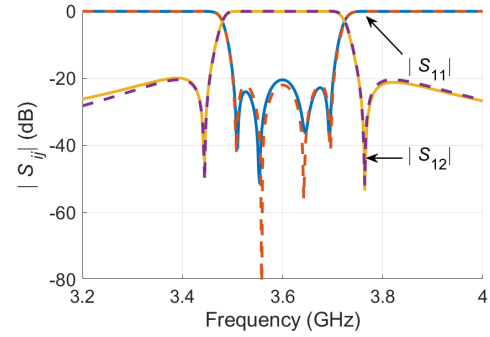


Fig. 12. Responses of synthesized dispersive coupling matrix (dashed lines) and EM model (solid lines) of a dispersive box with two symmetric TZs (TZ arrangement 5).

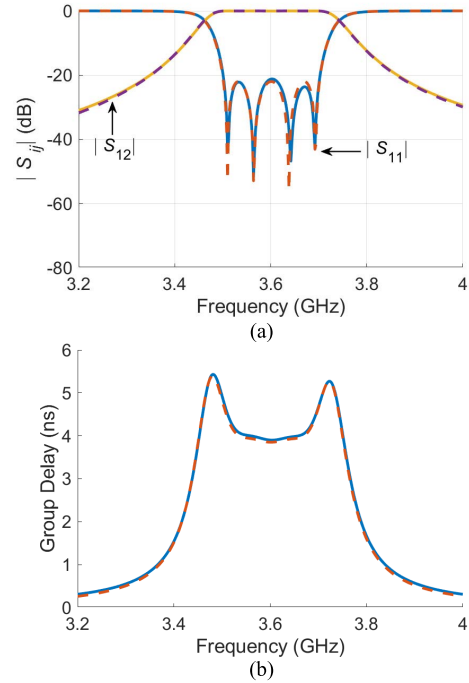


Fig. 13. (a) Magnitude and (b) group delay responses of synthesized dispersive coupling matrix (dashed lines) and EM model (solid lines) of a dispersive box with two complex conjugated TZs (TZ arrangement 6).

and fabricated to demonstrate the flexibilities in the arrangement and control of TZs of the dispersive box. An asymmetric response with one TZ in the low rejection band and three TZs in the high rejection band will be realized. Such an asymmetric response can hardly be realized utilizing the traditional cascaded MDR quadruplet structure without using the diagonal cross coupling. It will be demonstrated that applying the dispersive box structure can significantly reduce the manufacturing complexity and conveniently realize the desired near-passband response with a wide spurious-free high rejection band.

The ceramic material for the prototype MDR filter is with a relative permittivity of 19.15. The passband of the filter is from 3.36 to 3.62 GHz with the center frequency $f_0 = 3.488$ GHz and bandwidth $BW = 0.26$ GHz. The realized filter is with the size of $50 \times 24 \times 6$ mm. Four normalized TZs,

which are placed at $-2.6j$, $+1.12j$, $+1.38j$, and $+2.4j$, are specified in filter synthesis with the first two being assigned to the first dispersive box (1–2–3–4) and the second two being assigned to the second dispersive box (5–6–7–8), as narrated in Fig. 14(a). Note that the dispersive coupling element can be arbitrarily located in the dispersive box structure without changing the property of the topology due to the antisymmetry of the coupling structure. In the Appendix, the sufficient condition will be derived for a response that is realizable by cascading quasi-box sections with compatible coupling signs described in Section II. The resonant frequency range in this design example spans $[-1.1714, 1.0932]$, which satisfies the condition. Practically, the overall coupling matrix is obtained by a blockwise application of the transformation introduced in Section II. The coupling matrices in each step are as shown in the equations at the bottom of the page. The basic coupling matrix \mathbf{M}_1 with two CQ sections can be first synthesized according to the matured filter synthesis method.

With the equivalence in Fig. 2, two CQ sections can be first transformed into two quasi-box sections by (3) and (4), resulting in matrix \mathbf{M}_2 . Eventually, by blockwisely applying an analytic transformation (6), the overall dispersive coupling matrix \mathbf{M}_0 and \mathbf{M}_d can be obtained, where $\mathbf{M}_d(1, 2) = 0.5511$ and

$\mathbf{M}_d(7, 8) = 0.1875$. Rigorously speaking, regardless of different assignment of TZs, there are four solutions in total. However, only the one that has positive slopes in both dispersive boxes is realizable in the MDR filter. Accordingly, the design can be conducted with no ambiguity since there is a unique coupling matrix corresponding to the physical model that can be easily distinguished from the multiple solutions. The EM model that realizes the synthesized coupling matrix is shown in Fig. 14(b). The I/O coupling is realized by forming a partial height blind hole with inner surface metalized, which is isolated from the metalized outer surface of the filter by an unmetalized ring. The inner conductor of the external SMA connector is soldered inside the blind hole and the ground is bonded to the outer surface of the MDR filter.

The photograph of the prototyped eight-pole MDR filter is shown in Fig. 14(c) with the measured and synthesized narrowband responses shown in Fig. 15(a), demonstrating excellent agreement and further validating the TZ control capability of the dispersive box structure. The wideband responses of the measured and EM simulated are shown in Fig. 15(b), presenting a clear wide spurious mode free rejection band from 4 to 5 GHz, as expected. Note that the spike appearing in the low rejection band is mainly caused by the resonances of

$$\mathbf{M}_1 = \begin{pmatrix} 0 & 0.9894 & 0 & 0 & 0 & 0 & 0 & 0 & 0 & 0 \\ 0.9894 & 0.0161 & 0.8080 & 0 & -0.1379 & 0 & 0 & 0 & 0 & 0 \\ 0 & 0.8080 & 0.1304 & 0.5608 & 0.3312 & 0 & 0 & 0 & 0 & 0 \\ 0 & 0 & 0.5608 & -0.5903 & 0.4187 & 0 & 0 & 0 & 0 & 0 \\ 0 & -0.1379 & 0.3312 & 0.4187 & 0.0439 & 0.5418 & 0 & 0 & 0 & 0 \\ 0 & 0 & 0 & 0 & 0.5418 & 0.0612 & 0.5544 & 0 & 0.0983 & 0 \\ 0 & 0 & 0 & 0 & 0 & 0.5544 & -0.0042 & 0.3464 & 0.5389 & 0 \\ 0 & 0 & 0 & 0 & 0 & 0 & 0.3464 & -0.7360 & 0.6097 & 0 \\ 0 & 0 & 0 & 0 & 0 & 0.0983 & 0.5389 & 0.6097 & 0.0161 & 0.9894 \\ 0 & 0 & 0 & 0 & 0 & 0 & 0 & 0 & 0.9894 & 0 \end{pmatrix}$$

$$\mathbf{M}_2 = \begin{pmatrix} 0 & 0.9894 & 0 & 0 & 0 & 0 & 0 & 0 & 0 & 0 \\ 0.9894 & 0.0161 & -0.3872 & 0.7091 & -0.1379 & 0 & 0 & 0 & 0 & 0 \\ 0 & -0.3872 & -0.8966 & 0 & 0.2088 & 0 & 0 & 0 & 0 & 0 \\ 0 & 0.7091 & 0 & 0.4366 & 0.4914 & 0 & 0 & 0 & 0 & 0 \\ 0 & -0.1379 & 0.2088 & 0.4914 & 0.0439 & 0.5418 & 0 & 0 & 0 & 0 \\ 0 & 0 & 0 & 0 & 0.5418 & 0.0612 & 0.2052 & 0.5151 & -0.0983 & 0 \\ 0 & 0 & 0 & 0 & 0 & 0.2052 & -0.8740 & 0 & 0.3671 & 0 \\ 0 & 0 & 0 & 0 & 0 & 0.5151 & 0 & 0.1338 & -0.7262 & 0 \\ 0 & 0 & 0 & 0 & 0 & -0.0983 & 0.3671 & -0.7262 & 0.0161 & 0.9894 \\ 0 & 0 & 0 & 0 & 0 & 0 & 0 & 0 & 0.9894 & 0 \end{pmatrix}$$

$$\mathbf{M}_0 = \begin{pmatrix} 0 & 0.8256 & 0 & 0 & 0 & 0 & 0 & 0 & 0 & 0 \\ 0.8256 & -0.6172 & -0.8172 & 0.5917 & 0 & 0 & 0 & 0 & 0 & 0 \\ 0 & -0.8172 & -0.8966 & 0 & 0.2088 & 0 & 0 & 0 & 0 & 0 \\ 0 & 0.5917 & 0 & 0.4366 & 0.4914 & 0 & 0 & 0 & 0 & 0 \\ 0 & 0 & 0.2088 & 0.4914 & 0.0439 & 0.5418 & 0 & 0 & 0 & 0 \\ 0 & 0 & 0 & 0 & 0.5418 & 0.0612 & 0.2052 & 0.5151 & 0 & 0 \\ 0 & 0 & 0 & 0 & 0 & 0.2052 & -0.8740 & 0 & 0.3606 & 0 \\ 0 & 0 & 0 & 0 & 0 & 0.5151 & 0 & 0.1338 & -0.6882 & 0 \\ 0 & 0 & 0 & 0 & 0 & 0 & 0.3606 & -0.6882 & -0.2472 & 0.9719 \\ 0 & 0 & 0 & 0 & 0 & 0 & 0 & 0 & 0.9719 & 0 \end{pmatrix}$$

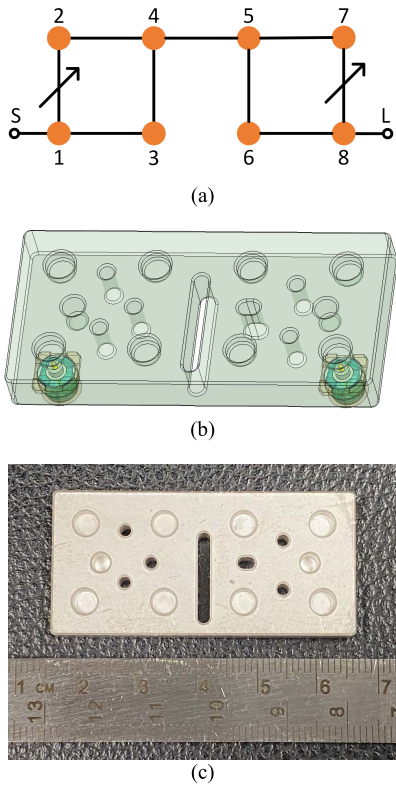


Fig. 14. Eight-pole asymmetric response MDR filter consisting of two cascaded dispersive box units. (a) Coupling topology. (b) EM model. (c) Photograph of the prototyped hardware.

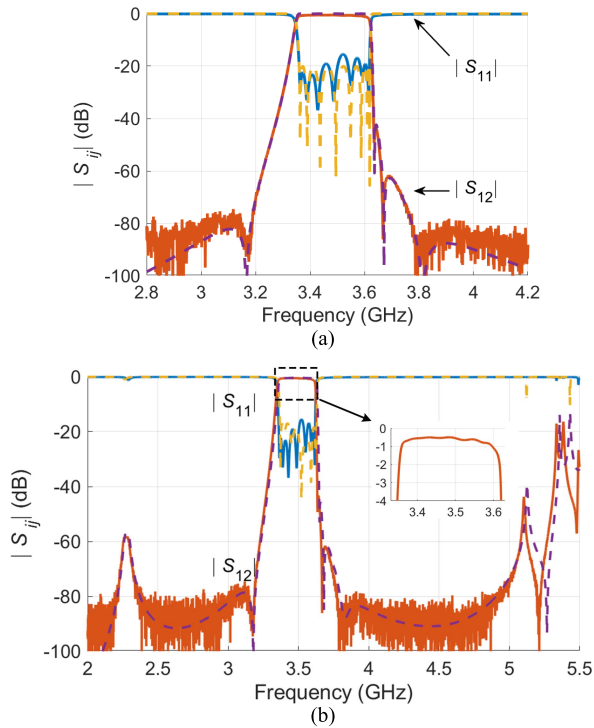


Fig. 15. (a) Narrowband responses of the measurement (solid lines) and synthesis (dashed lines). (b) Wideband responses of the measured response (solid lines) and the EM model (dashed lines).

the two blind holes for dispersive couplings. Although the level of the spike is low enough to satisfy the given specs, it can be

reduced by deliberately shifting the two resonant frequencies in the physical design. The in-band insertion loss shown in the figure is comparable to conventional metal coaxial resonator filters, which demonstrates the potential applicability of the MDR filter to future wireless communication systems.

VI. CONCLUSION

This article presents a comprehensive theory for synthesis and design of a bandpass filter that incorporates dispersive box coupling sections for realizing arbitrary 4–2 TZ arrangements of the sections, particularly, in realizing high-performance quasi-TEM mode MDR filters. Compared to the traditional CQ section structure, the dispersive box structure eliminates the manufacturing-inconvenient diagonal cross coupling while providing full control of the two TZs. In addition, the physical realization in MDR form of the coupling section naturally possesses a wide spurious mode free high rejection band. The mild sufficient condition for realizing an MDR bandpass filter with cascaded dispersive box sections is also derived, for which the coupling signs and the slope of the dispersive coupling are restricted. This condition states that none of the TZs should lie in between two resonant frequencies of the filter. The mathematical congruent transform provides the simple mapping between the coupling matrices of the traditional CQ structure and the dispersive box structure. An eight-pole quasi-TEM mode MDR filter that is composed of two cascaded dispersive boxes and with an asymmetric response is designed, fabricated, and measured to demonstrate the usefulness of the coupling structure, showing a high near-passband rejection response and a wide high rejection band. It is expected that the dispersive box structure will be a practical solution to lightweight and high-performance MDR filters for 5G and future wireless communication base stations.

APPENDIX

In this appendix, three useful propositions for synthesizing the dispersive box or quasi-box coupling topology will be proved. The first proposition is very general to all filter coupling matrices.

Proposition 1: Let \mathbf{M} be a real-valued symmetric matrix (typically a coupling matrix) and λ_{\max} (resp. λ_{\min}) be its maximal (resp. minimal) eigenvalue. Then,

$$\forall i, \quad \lambda_{\min} \leq M_{ii} \leq \lambda_{\max}. \quad (\text{A.1})$$

In other terms, all the diagonal elements of \mathbf{M} lie within the interval $[\lambda_{\min}, \lambda_{\max}]$.

Proof: As a real symmetric matrix, \mathbf{M} is diagonalizable in an orthonormal basis \mathbf{P} , meaning that $\mathbf{M} = \mathbf{P}^T \mathbf{\Lambda} \mathbf{P}$ with $\mathbf{P}^T \mathbf{P} = \mathbf{I}$. It can be found that

$$M_{ii} = \sum_k \lambda_i (P_{ki})^2 \leq \lambda_{\max} \sum_k (P_{ki})^2 = \lambda_{\max}. \quad (\text{A.2})$$

The left-hand side of inequality (A.1) can be obtained similarly. The result can also be seen as a consequence of the Rayleigh–Ritz theorem [27, p.176].

The second proposition is specific to quasi-box sections.

Proposition 2: Consider a quasi-box section with coupling matrix \mathbf{M} and define the real-valued interval $I = [\min(-M_{22}, -M_{33}), \max(-M_{22}, -M_{33})]$, where $-M_{22}$ and $-M_{33}$ are the

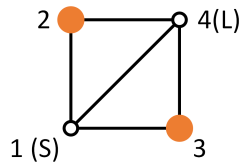


Fig. 16. Simplified quasi-box topology with resonators 1 and 4 in Fig. 2 (b) neglected and replaced with I/O ports.

two resonant frequencies of the quasi-box section. Suppose that none of the two TZ frequencies of the section lies in the interval I . In the case of simple or double TZs on the $j\omega$ axis, the zero's angular frequencies (i.e., the TZ values divided by j) lie outside the interval I , whereas in the case of a complex TZ pair, the hypothesis is automatically verified as their frequencies are not real-valued. Then,

$$M_{12}M_{24}M_{13}M_{34} \leq 0. \quad (\text{A.3})$$

In particular, upon a usual response-invariant sign change, an equivalent coupling matrix \mathbf{M}' exists where coupling (1–2) is negative, while couplings (2–4), (1–3), and (3–4) are positive.

Proof: The TZs of a quasi-box section can be fully described by the zeros of the simplified transversal section shown in Fig. 16. They are determined by the zeros of the transadmittance of the admittance matrix \mathbf{Y} that corresponds to the coupling matrix \mathbf{M}

$$Y_{12}(s) = \frac{M_{12}M_{24}}{s + jM_{22}} + \frac{M_{13}M_{34}}{s + jM_{33}} + jM_{14}. \quad (\text{A.4})$$

If terms $M_{12}M_{24}$ and $M_{13}M_{34}$ have the same sign, without loss of generality, for example, positive, then Y_{12} is a lossless admittance function (if negative take $-Y_{12}$) and its poles and zeros therefore alternate, implying that one of its zeros lie in the interval I , which provides a contradiction.

Now, a sufficient condition for realizing a bandpass filter with cascaded quasi-box sections or dispersive box sections can be drawn as follows.

Proposition 3: Let \mathbf{S} be a filter response with associated admittance matrix \mathbf{Y} . Denote by ω_i the poles of \mathbf{Y} that is the resonant frequencies of the system. Define the interval $J = [\min_i(\omega_i), \max_i(\omega_i)]$ and consider a coupling topology involving quasi-box sections in a cascaded fashion (possibly combined with other types of sections) chosen to realize \mathbf{S} . Suppose that none of the TZ frequencies assigned to quasi-box sections belongs to J . The proposition states that none of the TZs affected by quasi-box sections belongs to J . Under this mild hypothesis, the signs of the mutual couplings of each quasi-box section can be chosen as described in Proposition 2.

Proof: The result is a straightforward consequence of Propositions 1 and 2. Suppose that $\omega_{i=1,2}$ are two TZ frequencies associated with a quasi-box section embedded in a cascaded topology with global coupling matrix \mathbf{M} . The resonant frequencies are the opposite values of the eigenvalues of \mathbf{M} . By Proposition 1, the interval spanned by the eigenvalues of \mathbf{M} contains the interval spanned by the diagonal terms of the quasi-box section. This in turn implies Proposition 2.

ACKNOWLEDGMENT

The authors would like to thank Huawei Technologies Company Ltd. for sponsoring this research and Hua-Hong Wang of Huawei for useful suggestions throughout the research and fabricating the filter prototype.

REFERENCES

- [1] R. L. Sokola and C. Choi, "Ceramic bandpass filter," U.S. Patent 4431977, Feb. 14, 1984.
- [2] D. M. DeMuro and D. Agahi-Kesheh, "Monolithic ceramic filter with bandstop function," U.S. Patent 4823098, Apr. 18, 1989.
- [3] Y. Konishi, "Novel dielectric waveguide components-microwave applications of new ceramic materials," *Proc. IEEE*, vol. 79, no. 6, pp. 726–740, Jun. 1991.
- [4] K. Sano and M. Miyashita, "Dielectric waveguide filter with low profile and low-insertion loss," *IEEE Trans. Microw. Theory Techn.*, vol. 47, no. 12, pp. 2299–2303, Dec. 1999.
- [5] I. C. Hunter and M. Y. Sandhu, "Monolithic integrated ceramic waveguide filters," in *IEEE MTT-S Int. Microw. Symp. Dig. (IMS)*, Jun. 2014, pp. 1–3.
- [6] X. Wang and K. Wu, "A TM_{01} mode monoblock dielectric filter," *IEEE Trans. Microw. Theory Techn.*, vol. 62, no. 2, pp. 275–281, Feb. 2014.
- [7] B. Yuan, "Filter and transceiver comprising dielectric body resonators having frequency adjusting holes and negative coupling holes," U.S. Patent 9998163 B2, Jun. 12, 2018.
- [8] S. Tamiazzo and G. Macchiarella, "An analytical technique for the synthesis of cascaded N -tuplets cross-coupled resonators microwave filters using matrix rotations," *IEEE Trans. Microw. Theory Techn.*, vol. 53, no. 5, pp. 1693–1698, May 2005.
- [9] X. Zhang, B. Yuan, Z. Liu, and Z. Shen, "Dielectric filter, transceiver and base station," W.O. Patent 2017088174 A1, Jun. 1, 2017.
- [10] U. Rosenberg and S. Amari, "A novel band-reject element for pseudoelliptic bandstop filters," *IEEE Trans. Microw. Theory Techn.*, vol. 55, no. 4, pp. 742–746, Apr. 2007.
- [11] L. Szydlowski, A. Lamecki, and M. Mrozowski, "Coupled-resonator waveguide filter in quadruplet topology with frequency-dependent coupling—A design based on coupling matrix," *IEEE Microw. Wireless Compon. Lett.*, vol. 22, no. 11, pp. 553–555, Nov. 2012.
- [12] L. Szydlowski, N. Leszczynska, and M. Mrozowski, "Dimensional synthesis of coupled-resonator pseudoelliptic microwave bandpass filters with constant and dispersive couplings," *IEEE Trans. Microw. Theory Techn.*, vol. 62, no. 8, pp. 1634–1646, Aug. 2014.
- [13] Y. Zhang, H. Meng, and K.-L. Wu, "Direct synthesis and design of dispersive waveguide bandpass filters," *IEEE Trans. Microw. Theory Techn.*, vol. 68, no. 5, pp. 1678–1687, May 2020.
- [14] U. Rosenberg, S. Amari, and F. Seyfert, "Pseudo-elliptic direct-coupled resonator filters based on transmission-zero-generating irises," in *Eur. Microw. Conf. Dig.*, Sep. 2010, pp. 962–965.
- [15] Y. He et al., "A direct matrix synthesis for in-line filters with transmission zeros generated by frequency-variant couplings," *IEEE Trans. Microw. Theory Techn.*, vol. 66, no. 4, pp. 1780–1789, May 2018.
- [16] L. Szydlowski, N. Leszczynska, and M. Mrozowski, "Generalized Chebyshev bandpass filters with frequency-dependent couplings based on stubs," *IEEE Trans. Microw. Theory Techn.*, vol. 61, no. 10, pp. 3601–3612, Oct. 2013.
- [17] Y. Zhang, H. Meng, and K.-L. Wu, "Synthesis of microwave filters with dispersive coupling using isospectral flow method," in *IEEE MTT-S Int. Microw. Symp. Dig. (IMS)*, Jun. 2019, pp. 846–848.
- [18] S. Tamiazzo and G. Macchiarella, "Synthesis of cross-coupled filters with frequency-dependent couplings," *IEEE Trans. Microw. Theory Techn.*, vol. 65, no. 3, pp. 775–782, Mar. 2017.
- [19] Y. Zhang, F. Seyfert, S. Amari, M. Olivi, and K.-L. Wu, "General synthesis method for dispersively coupled resonator filters with cascaded topologies," *IEEE Trans. Microw. Theory Techn.*, vol. 69, no. 2, pp. 1378–1393, Feb. 2021.
- [20] L. Szydlowski, N. Leszczynska, A. Lamecki, and M. Mrozowski, "A substrate integrated waveguide (SIW) bandpass filter in a box configuration with frequency-dependent coupling," *Microw. Wireless Compon. Lett.*, vol. 22, no. 11, pp. 556–558, Nov. 2012.
- [21] R. J. Cameron, A. R. Harish, and C. J. Radcliffe, "Synthesis of advanced microwave filters without diagonal cross-couplings," *IEEE Trans. Microw. Theory Techn.*, vol. 50, no. 12, pp. 2862–2872, Dec. 2002.

- [22] Y. Zhang, Y. Chen, and K.-L. Wu, "A dispersive quadruplet structure for monoblock dielectric resonator filters," *IEEE Trans. Microw. Theory Techn.*, vol. 70, no. 6, pp. 3105–3114, Jun. 2022.
- [23] Y. Zhang, F. Seyfert, and K.-L. Wu, "Exhaustive synthesis and realization of extended-box topologies with dispersive couplings," in *IEEE MTT-S Int. Microw. Symp. Dig. (IMFW)*, Nov. 2021, pp. 33–35.
- [24] R. J. Cameron, J.-C. Faugere, F. Rouillier, and F. Seyfert, "Exhaustive approach to the coupling matrix synthesis problem and application to the design of high degree asymmetric filters," *Int. J. RF Microw. Comput.-Aided Eng.*, vol. 17, no. 1, pp. 4–12, Jan. 2007.
- [25] H. Hu and K.-L. Wu, "A generalized coupling matrix extraction technique for bandpass filters with uneven-Qs," *IEEE Trans. Microw. Theory Techn.*, vol. 62, no. 2, pp. 244–251, Feb. 2014.
- [26] R. J. Cameron, C. M. Kudsia, and R. Mansour, *Microwave Filters for Communication Systems: Fundamentals, Design, and Applications*, 2nd ed. Hoboken, NJ, USA: Wiley, 2018.
- [27] R. A. Horn and C. R. Johnson, *Matrix Analysis*, New York, NY, USA: Cambridge Univ. Press, 2012.



Yan Zhang (Member, IEEE) received the B.S. degree in electronic engineering from the University of Electronic Science and Technology of China, Chengdu, China, in 2017, and the Ph.D. degree from The Chinese University of Hong Kong, Shatin, Hong Kong, in 2022.

She is currently with Huawei Technologies Company Ltd., Shanghai, China. Her current research interests include synthesis and tuning of filters with dispersive couplings and filters with irregular topologies.



Fabien Seyfert received the B.Eng. degree from the Ecole Supérieure des Mines de St. Etienne, Saint-Étienne, France, in 1993, and the Ph.D. degree in mathematics from the Ecole Supérieure des Mines de Paris, Paris, France, in 1998.

From 1998 to 2001, he was with Siemens, Munich, Germany, as a Researcher specializing in discrete and continuous optimization methods. From 2002 to 2021, he was a Researcher with the Institut National de Recherche en Informatique et en Automatique (INRIA), Sophia Antipolis, France,

where he led the Functional Analysis for the Conception and Assessment of Systems (FACTAS) team. At the end of 2021, he took a leave from INRIA and started his own private research consultant activity. His research is focused on the development of efficient mathematical procedures and associated software for signal processing, including computer-aided techniques for the design and tuning of microwave devices.



Ke-Li Wu (Fellow, IEEE) received the B.S. and M.Eng. degrees from the Nanjing University of Science and Technology, Nanjing, China, in 1982 and 1985, respectively, and the Ph.D. degree from Laval University, Quebec, QC, Canada, in 1989.

From 1989 to 1993, he was with McMaster University, Hamilton, Canada, as a Research Engineer. He joined Com Dev International (now Honeywell Aerospace), Cambridge, ON, Canada, in 1993, where he was a Principal Member of Technical Staff. Since 1999, he has been with The Chinese University of Hong Kong, Hong Kong, China, where he is currently a Professor and the Director of the Radiofrequency Radiation Research Laboratory. His current research interests include EM-based circuit domain modeling of general electromagnetic problems, theory and practice of microwave filters, MIMO antenna arrays, and IoT technologies.

Prof. Wu is a member of the IEEE MTT-5 Filters Technical Committee. He was a recipient of the COM DEV Achievement Award in 1998 and the Asia-Pacific Microwave Conference Prize twice in 2008 and 2012, respectively. He was an Associate Editor of the IEEE TRANSACTIONS ON MICROWAVE THEORY AND TECHNIQUES from 2006 to 2009.

Prof. Wu is a member of the IEEE MTT-5 Filters Technical Committee. He was a recipient of the COM DEV Achievement Award in 1998 and the Asia-Pacific Microwave Conference Prize twice in 2008 and 2012, respectively. He was an Associate Editor of the IEEE TRANSACTIONS ON MICROWAVE THEORY AND TECHNIQUES from 2006 to 2009.